Pure Appl. Chem., Vol. 79, No. 1, pp. 21–37, 2007.
doi:10.1351/pac200779010021

Order and dynamics of rod-like and banana-shaped liquid crystals by ^{2}H NMR*

Valentina Domenici

Dipartimento di Chimica e Chimica Industriale, via Risorgimento 35, 56126 Pisa, Italy

Abstract: Deuterium NMR spectroscopy is a very powerful technique for studying partially or totally ordered systems, such as liquid crystals (LCs) and polymers. LCs represent a branch of the most general class of soft materials, with peculiar physical and chemical properties which attracted scientific attention for their potentiality for technological applications. From a chemical point of view, there are three aspects in which ^{2}H NMR could provide significant insights: (i) the conformational and structural properties; (ii) the molecular dynamics and mobility; and (iii) the orientational order and aggregation/distribution of molecules in the different liquid-crystalline phases. In this work, some of the recent developments in this field are discussed, focusing on two main topics: (1) the molecular dynamics of the smectic liquid-crystalline phases formed by rod-like molecules and (2) the unusual orientational and dynamic properties of the new liquid-crystalline mesophases formed by banana-shaped molecules (BLCs).

Keywords: liquid crystals; nematic; ferroelectric; smectic; NMR; deuterium; molecular dynamics; orientational order; banana-shaped molecules.

The field of liquid crystals (LCs) is one of the most fascinating aspects of the science of materials. On the other hand, deuterium nuclear magnetic resonance (^{2}H NMR) represents a very powerful spectroscopy for the large number of possibilities in performing and projecting new experiments and for enlightening the molecular structure, orientational ordering, and dynamics of LC molecules.

Among the various LCs, ferroelectric ones (FLCs), formed by rod-like mesogens, have dominated fundamental LC research for at least two decades [1,2], and their use for technological applications is now starting to have some relevant success [3]. Quite recently, new mesophases showing different levels of smectic order and chemical physical properties have found to be generated by banana-shaped molecules (BLCs) [4], and some of these smectic phases are very promising from a technological point of view [5], for instance, for optical processing devices, such as spatial light modulators, nonlinear optic, and wave-guide devices.

These are the main reasons for the interest in these materials from a technological point of view. However, for a chemist, LCs represent an extremely useful field to test molecular models, as well as to obtain parameters related to molecular properties, such as rotational diffusion coefficients (D_i) to describe the molecular dynamics.

Pure Appl. Chem.* **79, 1–65 (2007). A collection of invited, peer-reviewed articles by the winners of the 2006 IUPAC Prize for Young Chemists.

A typical way to study the dynamics at the molecular level is by analyzing ^{2}H relaxation times [6] by means of suitable theoretical models [7]. This procedure has been applied for several rod-like, or calamitic, LCs in their nematic and smectic A (SmA) phases, and recently, thanks to an extension of the theoretical treatment in order to be applied to biaxial phases [8], dynamic parameters have been obtained in the ferroelectric chiral smectic C (SmC*) phase.

The developments performed in the data analysis procedure, as well as the possibility to have different labeled isotopomers and frequency dependence measurements, allowed us to obtain the diffusion coefficient for the overall molecular motion named "tumbling motion" ($D_\perp$) unambiguously.

In the effort to overcome the problem of the indeterminacy of $D_\perp$, in the cases in which a small set of NMR data is available, the comparison between NMR and other experimental methods, such as dielectric relaxation [9,10] and neutron scattering (NS) [11], has been taken into account. Moreover, the comparison among different techniques is useful for testing theoretical models commonly used to extract dynamic information.

While in the case of rod-like LCs, most of the molecular and mesophase properties have been widely investigated by ^{2}H NMR [12], the LCs formed by BLCs, which have been recently discovered, still have some aspects to be understood, and ^{2}H NMR spectroscopy promises to be a useful tool for investigating the peculiar BLC mesophases.

Quite surprisingly, even the isotropic phase of BLC compounds turned out to have very unusual properties. ^{2}H NMR line widths and spin–spin relaxation times (T_2) recorded in the isotropic phase of several banana-shaped mesogens demonstrated that the molecular dynamics of these systems is particularly slow. An explanation of this behavior in terms of molecular hindering, or clustering, could be drawn on the basis of ^{2}H NMR experiments [13,14], in agreement with other recent experimental results [15,16].

Another interesting aspect of the BLC mesophases concerns the origin of the mesophase chirality, which seems to be strongly related to the molecular chirality. Despite the absence of chiral carbon centers, these molecules may assume a propeller-like conformation, as several works have proposed [17,18]. This molecular feature, called "atropoisomerism", may justify the occurrence of chirality in BLC mesophases.

In this paper, the contribution coming from ^{2}H NMR studies, which has been used for the first time to study molecular, structural, ordering, and dynamic properties of BLCs, is discussed in the framework of recent achievements.

Most of the results reported here are based on two banana-shaped mesogens [19], only differing for one substituent on the central ring (chlorine in the place of hydrogen). A first observation concerns the sensitivity of BLC systems to single substitutions: in fact, the presence of a chlorine atom determines the occurrence of a nematic phase instead of the B_2 phase. The nematic phase formed by these molecules is very peculiar with respect to the nematic phase formed by calamitic compounds, for the orientational order, molecular aggregation, phase symmetry, and dynamic behavior, as several ^{2}H NMR works have pointed out [20–23]. ^{2}H NMR spectroscopy provided interesting results for the orientational properties of the ferroelectric smectic B_2 phase [24] as well.

ORIENTATIONAL ORDER IN LIQUID CRYSTALS BY ^{2}H NMR

Ordered systems

LCs may be distinguished from other systems by the existence of a long-range orientational order with respect to an axis of preferred orientation, named the director, **n**.

The ordering of molecules in the LC mesophase [6] can be described by the orientational distribution function $f(\alpha,\beta,\gamma)$, namely, the probability of finding a molecule at a particular orientation defined by the Eulerian angles (α,β,γ) [25].

The distribution function $f(\alpha,\beta,\gamma)$ can be expanded in terms of the Wigner rotation matrices of rank L, $D^L_{n,m}(\alpha,\beta,\gamma)$, multiplied by the microscopic order parameters, $\langle D^{L*}_{n,m}(\alpha,\beta,\gamma)\rangle$ [26]:

$$f(\alpha,\beta,\gamma) = \sum_{L=0}^{\infty} \sum_{m,n=-L}^{L} \frac{2L+1}{8\pi^2} \left\langle D^{L*}_{n,m}(\alpha,\beta,\gamma) \right\rangle \cdot D^L_{n,m}(\alpha,\beta,\gamma) \tag{1}$$

Depending on the symmetry of both of the mesophases and the molecules themselves, this function can be simplified, as in the case of molecules approximated to cylindrical rods in a nematic phase. In this situation, $f(\alpha,\beta,\gamma)$ depends only on the angle β, and it can be truncated at $L = 2$, giving the expression $f(\beta) = {}^1\!/_2 + {}^5\!/_2\, P_2(\cos\beta) \cdot \langle P_2(\cos\beta)\rangle$, where $P_2(\cos\beta)$ is the Legendre polynomial and $\langle P_2(\cos\beta)\rangle$ is the nematic order parameter, S [26,27]. This quantity can be experimentally determined by different spectroscopic methods, such as NMR.

An alternative definition for order parameters can be obtained by expanding $f(\alpha,\beta,\gamma)$ in terms of the director cosines [27]. According to the ordering matrix formalism, the microscopic orientational order parameters can be related to the so-called Saupe ordering matrix components [28], $S_{ij}^{\lambda\mu} = \frac{1}{2}\langle 3i_\lambda j_\mu - \delta_{ij}\rangle$, where $i,j = (x,y,z)$ are the main axes in the molecular frame (MOL), $\lambda,\mu = (X,Y,Z)$ are the main axes in the LAB frame, and i_λ and j_μ are the direction cosines.

In the simplest case, represented by a uniaxial phase (e.g., the nematic phase) and rigid molecules having a cylindrical symmetry, the nematic order parameter corresponds to the S^{ZZ}_{zz} Maier–Saupe matrix element [26].

A complete treatment of the orientational order in LCs can be found in refs. [26,27,29].

Smectic phases have an additional order, which is called positional order. In the SmA phase, for instance, there is a one-dimensional translational periodicity, due to the fact that the centers of mass of the molecules tend to lie on planes normal to the director (Fig. 1).

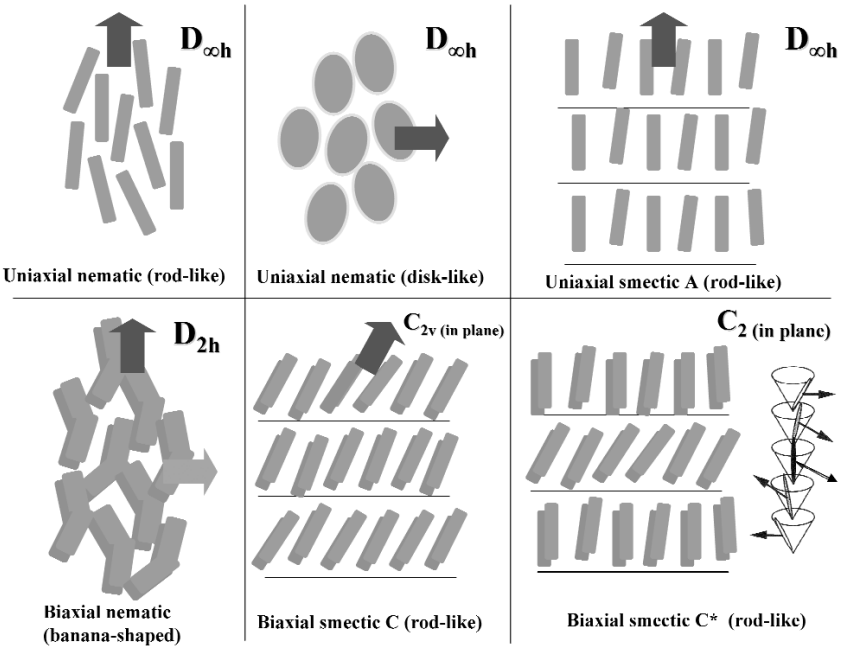

Fig. 1 Scheme of several liquid-crystalline phases formed by rod-like, disk-like, and BLCs. The phase symmetry and the main direction of the phase director (**n**) are shown.

In these mesophases, the orientational distribution function of a molecule is much more complicated than in the nematic phase, because it depends in principle on purely orientational and translational order parameters, but also mixed order parameters [26].

^{2}H NMR for studying orientational order in liquid crystals

^{2}H NMR is a very powerful technique for studying ordered systems, such as LCs, since the main contribution to the Hamiltonian is the quadrupolar interaction, due to the deuterium (nuclear spin I equal to 1). A general expression of the quadrupolar Hamiltonian is [30,31]:

$$\hat{H}_Q = \vec{I} \cdot \hat{Q} \cdot \vec{I} = \frac{eQ}{2I(2I-1)} \vec{I} \cdot \hat{V} \cdot \vec{I} \tag{2}$$

where eQ is the electric quadrupole moment and $\hat{V}$ is the local field gradient tensor, which is symmetric and diagonal in the C–D frame (with b axis collinear with the C–D bond and elements V_{aa}, V_{bb}, and V_{cc}).

The observed ^{2}H NMR spectrum in the simplest case of an oriented LC sample, with a single and isolated C–D bond, is characterized by a quadrupolar splitting, $\Delta\nu$, which can be written as:

$$\Delta\nu = \frac{3}{2} q_{bb} \left[S_{bb} + \frac{\eta}{3} \left(S_{cc} - S_{aa} \right) \right] \tag{3}$$

where $q_{bb} = \frac{eQV_{bb}}{\hbar}$ is the quadrupolar coupling constant and $\eta = \frac{V_{aa} - V_{bb}}{V_{cc}}$ is the asymmetry parameter.

Equation 3 relates the observed quadrupolar splitting with the orientational order parameters, S_{ii}, referred to the principal axes frame (PAS) defined by the three axes a,b,c in the C–D frame. Depending on the geometry of the molecular fragment where the C–D bond is located, after proper coordinate transformations, these parameters (PAS) can be related to the molecular order parameters (MOL).

As a general remark, the relation between the observed quadrupolar splitting and the molecular orientational order parameters is much more complex the more flexible is the molecule and the lower is the symmetry of the mesophase. Several theoretical models and data analysis procedures have been developed to overcome this limit [6,32].

In the following, the orientational order parameters of rigid fragments, typically phenyl and biphenyl moieties, will be reported for several rod-like mesogens in their mesophases.

DYNAMICS IN LIQUID CRYSTALS BY ^{2}H NMR

Dynamics by different spectroscopic techniques

Information on motional processes at a molecular level can be obtained by different spectroscopic techniques, such as NMR, dielectric spectroscopy (DS), and NS. However, the results so achieved are not easily comparable for several reasons: first, some techniques directly detect the time correlation functions, while others can only reveal their Fourier transforms, namely, the spectral densities, at a small number of frequencies. The second reason concerns the time window explored by these techniques, which determines the particular molecular model suitable for describing the observed quantities in terms of dynamic parameters. Another important difference among spectroscopic techniques is the rank of the operators associated to the investigated physical properties.

The intrinsic time scale (τ_{in}) of a technique depends on the physics of the phenomenon under observation. The τ_{in} represents the lowest limit below which a dynamic process is not detectable. For example, the electron spin resonance (ESR) spectral line shape is influenced by molecular reorienta-

tions, since the characteristic ESR τ_{in} is about 10^{-9} s. Differently, these motions are fast with respect to the ^{2}H NMR time window (~ 10^{-4}–10^{-5} s), thus, the ^{2}H NMR spectral line shape is only given by an average over all molecular reorientations.

Knowing the time scale of a spectroscopic technique is then important to select the appropriate theoretical model for interpreting the experimental observables in terms of dynamic properties. In particular, the τ_{in} typical of a technique must be compared with the time characteristic of the motion under study, defined the correlation time τ_c.

A significant example is given again by ESR and ^{2}H NMR used to study the molecular rotational motions in LCs ($\tau_c \sim 10^{-9}$ s): while the former requires the formalism of the stochastic Louiville equation, since the experiments fall in the *slow-motion* regime ($1 << \omega\tau_c$), the latter falls in the extreme narrowing regime ($1 >> \omega\tau_c$) and is better described by the Redfield theory.

All this considered, a spectroscopic technique could be more suitable to characterize a specific motion than another one, even though more frequently different techniques cover the same time window and/or overlap in certain ranges of time scale.

The molecular motions in thermotropic LCs [33] can be roughly divided into *translational diffusion* processes, involving the motion of the centers of mass of the molecules and *reorientational* processes of the molecule itself.

One fundamental point in the description of the stochastic processes in liquid-crystalline systems is the assumption that the translational and orientational motions are decoupled and that, consequently, they can be treated independently. This is supported by the experimentally observed different time scales [33] relative to the two kinds of motions.

Less evident is the possibility of separating overall molecular motions from conformational internal ones, since both of them usually take place on a similar time scale, giving rise to a quite complicated molecular dynamics [34] mechanism.

Groups of molecules also experience collective motions, in which the spatial average orientation of molecules fluctuates slowly compared to the much faster reorientational motions of the single molecules.

The role played by ^{2}H NMR

Deuterium represents the nucleus most widely used for obtaining dynamic information on LC systems. As previously mentioned, the time scale for ^{2}H NMR spectra is quite long, so that the line shapes are not sensitive to rotational motions. Single-pulse or quadrupolar-echo-pulse sequences are used in particular cases to detect the translational diffusion motions of LC molecules [35]. On the other hand, specific pulse sequences can be applied to measure relaxation times (five independent relaxation times, for nuclei with $I = 1$ as deuterium), each defining specific dynamic windows suitable to investigate different motions [36].

In particular, the two spin-lattice relaxation times, T_{1Z} and T_{1Q}, measured by using specific pulse sequences, are particularly sensitive to motions with correlation times of the same order of magnitude than the inverse of the Larmor frequency, i.e., in the range of 10^{-11}–τ_c–10^{-7} s in the case of a high magnetic field (B > 5T).

The three spin–spin relaxation times can be related to motions in a slower regime. The quadrupolar echo sequence [37], for instance, can detect motions with a correlation time in the range of 10^{-8}–τ_c–10^{-4} s, corresponding to the inverse of the quadrupolar coupling constant. Slower dynamic processes, up to $\tau_c \sim 10$ s, such as the order director fluctuations (ODFs) [38], can be studied by the Carr–Purcell–Meiboom–Gill (CPMG) pulse train sequence [39].

Moreover, several efforts have been spent to study different mechanisms of reorientation of molecules in the LC phases. An example is given by two-dimensional NMR experiments, where the spin-

lattice relaxation times T_1 are linked to the spin–spin relaxation times T_2 [36]. Thus, by combining different techniques to measure ^{2}H NMR relaxation times, a broad dynamic range can be covered.

ORIENTATIONAL ORDERING PROPERTIES OF ROD-LIKE LIQUID CRYSTALS

The case of the smectogen (+)-(*S*)-4-[4'-(1-methylheptyloxy)] biphenyl 4-(10-undecenyloxy) benzoate (11EB1M7) is here reported, as a representative example of ^{2}H NMR study of the orientational order of an LC having a rich variety of mesophases [40].

This rod-like smectogen (see Fig. 2) has a molecular structure formed by a rigid core, given by the aromatic fragment (phenyl and biphenyl units), and two long lateral chains, which represent the flexible parts of the molecule. This is typical of rod-like, or calamitic, LCs, where each component, the rigid and the flexible ones, are fundamental in order to get liquid-crystalline behavior. Moreover, this molecule possesses a chiral carbon, thus giving chiral mesophases, such as the cholesteric, the TGBA, and the SmC* phases.

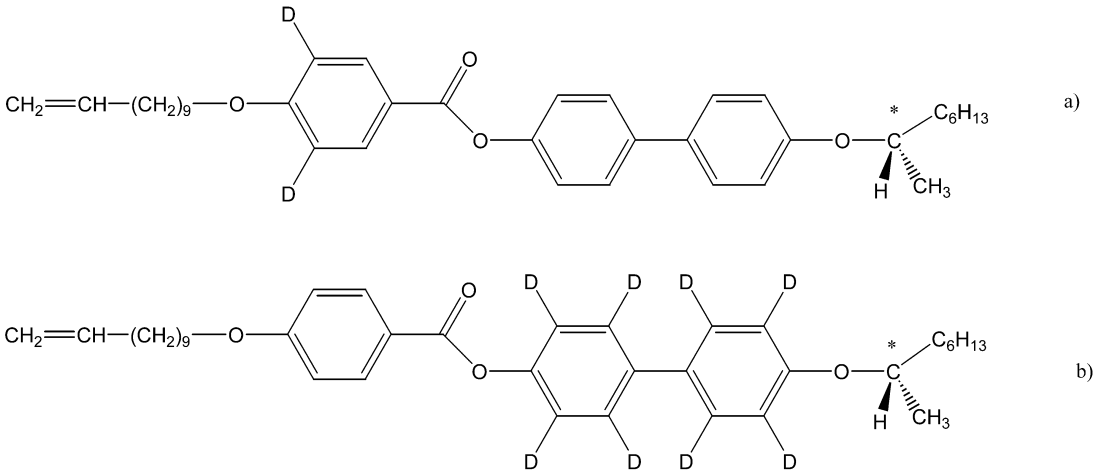

Fig. 2 Molecular structure of two deuterium-labeled isotopomers of the rod-like LC (+)-(*S*)-4-[4'-(1-methylheptyloxy)]biphenyl 4-(10-undecenyloxy)benzoate (11EB1M7): (a) 11EB1M7-d_2; (b) 11EB1M7-d_8.

In this study, two selectively labeled samples were available, one labeled on the biphenyl (11EB1M7-d_8) and the other one on the phenyl ring (11EB1M7-d_2), as shown in Fig. 2.

This selectivity allowed us to obtain independently the two local order parameters S_{zz} relative to the *para* axes of the two aromatic fragments. In fact, both the phenyl and the biphenyl units can be assumed to have a C_{2v} symmetry due to the fast rotation around the *para* axes.

Two orientational order parameters, namely, the principal order parameter $S_{zz}(T)$ and the fragment biaxiality $\Delta_{biax}(T) = S_{xx}(T) - S_{yy}(T)$, can be determined for each fragment.

The experimental quadrupolar splittings for the deuterons of 11EB1M7-d_2, as well as 11EB1M7-d_8, are connected to these local order parameters according to the following equations, which can be derived from eq. 3, by passing from the *abc* frame (PAS) to the *xyz* local fragment frame (with *z* along the *para* axis) [12]:

$$\Delta\nu_q\left[T\right]=\frac{3}{2}q_{bb}\left\{S_{zz}\left[T\right]\cdot\left(\cos^2\phi-\frac{1}{2}\sin^2\phi-\frac{\eta}{6}\cos^2\phi+\frac{\eta}{6}+\frac{\eta}{3}\sin^2\phi\right)+\Delta_{\text{biax}}\left(\frac{1}{2}\sin^2\phi+\frac{\eta}{6}\cos^2\phi+\frac{\eta}{6}\right)\right\} \tag{4}$$

The standard values of q_{bb} = 185 kHz and η = 0.04 have been used in the analysis; ϕ is the angle between the C–D bond and the z direction (*para* axis) and it has been assumed equal to 60°.

By analyzing the experimental data, the order parameters S_{zz} of the two fragments have been determined, and their values in the different mesophases are reported in Table 1. The value of the fragment biaxiality has been found to be very small for the phenyl ring and almost 0 for the biphenyl, according to the literature.

Table 1 The local orientational order S_{zz}, as defined in eq. 4, and the tilt angle θ (°), evaluated from ^2H NMR measurements for several rod-like LC mesogens.

Mesogen	S_{zz} in the nematic	S_{zz} in the SmA	S_{zz} in the SmC*	Limiting tilt angle, SmC*	S_{zz} in the Sm_{HEX}	Limiting tilt angle, Sm_{HEX}
11EB1M7-phen-D_2 [40]	/	0.67–0.73	0.73–0.66	18°	0.73–0.76	/
11EB1M7-biph-D_2 [40]	/	0.64–0.68	0.68–0.60	18°	0.88–0.89	/
HAB-phen-D_4 [41]	0.55–0.75	0.75–0.82	/	/	/	/
8BEF5-phen-D_4 [42]	/	0.70–0.85	0.85–0.81	11°	0.86–0.94	5–6°
MBHB-biph-D_8 [43]	/	0.70–0.86	0.86–0.83	28°	0.85–0.90	5°
10B1M7-phen-D_2 [44]	/	0.69–0.74	0.73–0.64	21°	0.88–0.90	/
10B1M7-biph-D_2 [44]	/	0.62–0.65	0.64–0.51	21°	0.59–0.74	/

To have an idea of these quantities, the order parameters S_{zz} (referred to the *para* axes of the labeled phenyl or biphenyl units) of several smectogens studied by ^2H NMR are reported in Table 1. These values are quite indicative of the overall molecular order parameters, since they are mostly determined by the rigid core of LCs.

The investigated rod-like LC mesogens are the non-chiral *p*-di-*n*-heptylazoxybenzene (HAB) [41] and the chiral mesogens (*S*)-[4-(2-methylbutyl)phenyl]-4'-*n*-octylbiphenyl carboxylate (8BEF5) [42], (*S*)-[4-(2-methylbutyloxycarbonyl)phenyl]-4'-*n*-heptylbiphenyl carboxylate (MBHB) [43], and (*S*)-1-methylheptyl-4'-(4''-*n*-decyloxybenzoyloxy)biphenyl-4-carboxylate (10B1M7) [44].

As a general remark, Table 1 shows that the order parameter S_{zz} increases by decreasing the temperature in the nematic, SmA and not tilted hexatic phases, while it decreases in tilted phases, due to the increasing of the tilt angle until reaching the limiting value, which is indicated in Table 1, for tilted phases.

In the SmC* phase, the tilt angle is due to the occurrence of a supramolecular organization of molecules within the phase (see Fig. 1): molecules are distributed in layers, and the local director is tilted in respect to the normal to the layer; moving from a layer to the next one, the local director of the phase describes an helicoidal structure. In the presence of the magnetic field, the helical axis orients parallel to the field, and if the helicoidal structure is not unwound by the field [45], the tilt angle θ can be evaluated from ^2H NMR by using the following formula:

$$S_{zz}^{\text{exp}}=\left(\frac{3\cos^2\theta-1}{2}\right)S_{zz}^{\text{calc}} \tag{5}$$

where S_{zz}^{exp} is the parameter obtained from ^2H NMR quadrupolar splitting, according to eq. 4, in the SmC*, and S_{zz}^{calc} is obtained by extrapolating the trend of S_{zz} from the SmA phase.

So far, in the examined cases, the value of tilt angle θ has been found to be temperature-dependent, according to the Landau–de Gennes equation [46]:

$$\theta = \theta^* \left[\left(T_0 - T \right) / T_0 \right]^{\gamma} \tag{6}$$

The values reported in Table 1 confirm that ^{2}H NMR spectroscopy can be used to determine this important feature. Moreover, the tilt angles obtained by NMR agree with those obtained by other techniques, such as X-rays and optical measurements.

REORIENTATIONAL DIFFUSION COEFFICIENTS IN UNIAXIAL PHASES

In addition to the orientational order parameters and mesophase features, other interesting aspects are related to the molecular mobility and dynamics. As previously mentioned, ^{2}H NMR can provide detailed information from the measurement of spin-lattice relaxation times, namely, T_{1Z} and T_{1Q}. As a general result, the measured ^{2}H spin-lattice relaxation times in the SmA phase are of the order of tens of milliseconds, and their trend within the temperature indicates a motional narrowing regime ($\omega_0 \tau_c << 1$) for the motions mainly contributing to the relaxation.

This feature has been observed for several smectogens investigated so far [34,47].

Dynamic information is contained in the spectral densities, which can be calculated from the experimental relaxation times in the Redfield theory approximation [48], through the following relationships:

$$J_1\left(\omega_0\right) = \frac{1}{3T_{1Q}} \tag{7}$$

$$J_2\left(2\omega_0\right) = \frac{1}{4T_{1Z}} - \frac{1}{12T_{1Q}} \tag{8}$$

where ω_0 is the Larmor frequency.

However, the extraction of quantitative dynamic parameters is not straightforward, due to the complexity of the molecular models describing molecular motions [7,34]. Several of them have been developed to describe the overall molecular reorientations in uniaxial phases, such as the nematic and SmA ones. The model mainly used is that proposed by Nordio et al. [49].

According to this model, the spectral densities can be related to correlation times, τ, which can be in turn written as a function of the diffusion coefficients for the spinning ($D_{//}$) and tumbling ($D_{\perp}$) motions (see Fig. 3). Internal motions (D_R) of the aromatic fragments and overall molecular motions ($D_{//}$ and $D_{\perp}$) are usually considered decoupled, and the internal motions affecting the aromatic rings are usually described in an isotropic potential by means of the small step diffusion [50,51] or the strong collision [52] models.

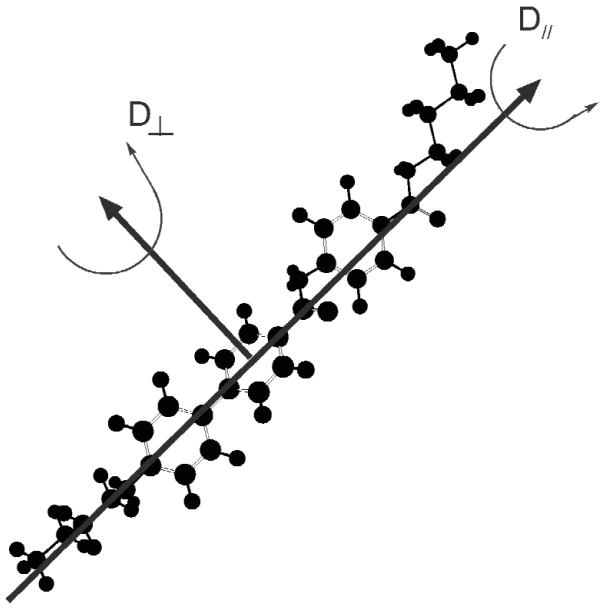

Fig. 3 Overall molecular motions and relative diffusion coefficients: spinning (//) and tumbling (⊥) reorientational motions for the rod-like molecule of 11EB1M7.

The resulting expressions for the spectral density and the correlation time are [6]:

$$J^i_{m_L}\left(m_L\omega_0\right)=\frac{3}{8}\left(q_{bb}\right)^2\sum_{m_M=-2}^{2}\sum_{m_R=-2}^{2}c_{m_Lm_M}\left[d^2_{m_R0}\left(\beta_{i,Q_i}\right)\right]^2\left[d^2_{m_Mm_R}\left(\beta_{M,i}\right)\right]^2$$
$$\sum_j a^{(j)}_{m_Lm_M}\frac{\left(\tau^{(j)}_{m_Lm_M}\right)^{-1}+\xi\left(m_R\right)D_i}{\left(m_L\omega_0\right)^2+\left[\left(\tau^{(j)}_{m_Lm_M}\right)^{-1}+\xi\left(m_R\right)D_i\right]^2} \tag{9}$$

and

$$\frac{1}{\tau^{(j)}_{m_Lm_M}}=\frac{6D_\perp}{b^{(j)}_{m_Lm_M}}+m_M^2\left(D_{//}-D_\perp\right) \tag{10}$$

where $d_{rs}{}^2$ are the reduced Wigner matrices, $\beta_{i,Qi}$ is the angle between the C–D bond and the axis about which the internal rotation occurs, $\beta_{M,i}$ is the angle between this axis and the molecular long axis, D_i is the diffusion coefficient relative to the internal rotation of the fragment considered, and $\zeta(_{\mathrm{mR}})$ is $(1 - \delta_{\mathrm{mR}})$ or $\mathrm{m_R}^2$ if strong collision or small step diffusion models are used, respectively.

The coefficients $a_{m_Lm_M}$, $b_{m_Lm_M}$, and $c_{m_Lm_M}$ are expressed [7] as a function of the principal order parameter S_{zz} for a Maier–Saupe potential, experimentally obtained from ^{2}H NMR.

The experimental spectral densities obtained by ^{2}H NMR can be fitted by eq. 9 to extract dynamic parameters. However, due to the complexity of this equation and the number of parameters involved, a global target fitting procedure is needed for analyzing ^{2}H relaxation times [53]. This approach requires that the diffusion coefficients are temperature-dependent. An example is given by the Arrenhius trend:

$D(T) = D^{\infty} \exp[-\Delta E_a/(RT)]$, where two parameters ($D^{\infty}$ and ΔE_a) are needed to describe a single motion.

However, several studies [54,55] enlighten the fact that the diffusion coefficient for the tumbling motion ($D_{\perp}$) is not well determined, but only an upper limiting value could be estimated. The first way to overcome this indetermination consists in fixing the ratio between the spinning and tumbling coefficients ($D_{//}/D_{\perp}$), according to the Perrin model [56].

In recent years, several alternative procedures were tested to get self-consistent ^{2}H NMR data analysis:

- recording relaxation data at different angles between the magnetic field and the local phase director [57];
- analyzing relaxation data of different labeled isotopomers with a single global target fitting [40,58,59];
- recording relaxation data at different Larmor frequencies [60];
- comparing relaxation ^{2}H NMR data with those obtained from dielectric relaxation experiments [9,10].

All these possibilities have been carried out, and the values of the diffusion coefficients reported in Table 2 refer to self-consistent ^{2}H NMR data analyses.

Table 2 Rotational diffusion coefficients (s^{-1}) and activation energies (kJ/mol) for the spinning, tumbling, and internal motions, determined from ^{2}H NMR data analysis for several rod-like smectogens in the SmA phase. The values of D are taken at a temperature T in the middle of the temperature range of stability ΔT of the SmA phase.

Mesogen	$D_{//}$ in the SmA	$D_{\perp}$ in the SmA	D_R in the SmA	ΔE_a (//) in SmA	ΔE_a ($\perp$) in SmA	ΔE_a (R) in SmA
11EB1M7-phen-D_2 [60]	1.5×10^9	1.3×10^8	1.5×10^9	35.0	40.0	35.0
11EB1M7-biph-D_2 [60]	1.5×10^9	1.3×10^8	3.5×10^9	35.0	40.0	20.0
HAB-phen-α-D_4 [9]	1.3×10^9	1.5×10^7	1.1×10^9	25.5	39.2	35.0
HAB-phen-β-D_4 [9]	1.3×10^9	1.5×10^7	2.1×10^9	25.5	39.2	35.0
8BEF5-phen-D_4 [8]	7.9×10^8	1.1×10^8	1.9×10^{10}	29.6	29.6	33.3
MBHB-biph-D_8 [61]	2.5×10^9	5.0×10^8	3.2×10^9	32.1	32.1	29.1
10B1M7-phen-D_2 [59]	1.3×10^9	3.0×10^8	1.3×10^9	40.0	40.0	35.0
10B1M7-biph-D_2 [59]	1.3×10^9	3.0×10^8	3.5×10^9	40.0	40.0	40.0

As a general remark, the diffusion coefficients obtained for the spinning and tumbling molecular motions, as well as for the internal motions of the phenyl and biphenyl groups, reported in Table 2, show similar trends. In particular, the tumbling motion is, in general, one or two orders of magnitude smaller than the spinning motion. As far as the internal motions of the aromatic fragments are concerned, a satisfactory reproduction of the experimental data by using a global target fitting procedure could not be achieved with the small step rotational diffusion model, on the contrary, the strong collision model was successful for both the biphenyl and phenyl fragments.

This seems to be a general conclusion in ferroelectric (chiral) LCs, whilst in thermotropic LCs not exhibiting ferroelectric phases, both models are found to well describe the internal reorientations.

REORIENTATIONAL DIFFUSION COEFFICIENTS IN FERROELECTRIC SMECTIC PHASES

Although only uniaxial phases have been considered in the discussion so far, one of the most interesting phases in the field of thermotropic LCs is the smectic C* (SmC*), namely, the ferroelectric phase, which is biaxial. The practical difficulties in applying theoretical models to biaxial phases has prevented

for many years the analysis of relaxation times in the SmC* phase. To this aim, a new theoretical approach has been recently proposed by Veracini's group [8], and its application to several sets of data for different smectogens is here discussed. This new approach allows us the quantitative analysis of relaxation times in tilted smectic phases by means of the existing theoretical models, neglecting the dependence of the relaxation times on the azimuthal angle ϕ, but taking into account the effects of the tilt angle ϕ. This statement is based on both experimental and theoretical reasons.

In SmC* phases, the phase director **n** describes a helicoidal structure along the normal to the smectic planes (z axis) (i.e., the tilt angle θ between **n** and z do not change), while the azimuthal angle ϕ assumes different values depending on the z coordinate. Relaxation times depend in principle on both angles. However, from the experimental point of view, equivalent deuterons of different molecules in different planes and, therefore, with different ϕ, have exactly the same quadrupolar splitting, thus with indistinguishable results. Moreover, a single relaxation decay can be recorded due to the average over all molecules. The experimental evidence of a mono-exponential decay for all the ^2H spin-lattice measurements performed so far in tilted smectic phases indicates that, if any ϕ-dependence is present, it would be nevertheless so small as to be undetectable.

On the other hand, even if different experimental values for the relaxation times could be obtained for different ϕ values, no suitable theoretical models are actually available to analyze them in terms of dynamic parameters.

By neglecting the dependence on ϕ, the relaxation data recorded in the SmC* phase could be analyzed [8], and the results for several smectogens [8,10,61] are reported in Table 3.

Table 3 Rotational diffusion coefficients (s^{-1}) and activation energies (kJ/mol) for the spinning, tumbling, and internal rotations, determined from ^2H NMR data analysis for several rod-like smectogens in the SmC* phase. The values of D are taken at a temperature T in the middle of the temperature range of stability ΔT of the SmC* phase.

Mesogen	$D_{//}$ in the SmC*	$D_{\perp}$ in the SmC*	D_R n the SmC*	ΔE_a (//) in SmC*	ΔE_a ($\perp$) in SmC*	ΔE_a (R) in SmC*
11EB1M7-phen-D_2 [10]	1.2×10^9	1.1×10^7	4.1×10^8	20.0	119.0	78.0
11EB1M7-biph-D_2 [10]	1.2×10^9	1.1×10^7	1.5×10^9	20.0	119.0	61.0
8BEF5-phen-D_4 [8]	1.0×10^9	1.1×10^8	7.2×10^9	70.0	70.0	19.0
MBHB-biph-D_8 [61]	1.2×10^9	2.3×10^8	1.1×10^9	52.0	52.0	36.0

Some conclusions can be drawn by comparing the results shown in Tables 2 and 3 for the same smectogens:

1. The activation energy for the tumbling and spinning motions increases, passing from the SmA to the SmC* phases, except for the spinning motion of the 11EB1M7 smectogen.
2. No discontinuities could be observed passing from the SmA to the SmC* phases in the trend of the diffusion coefficients, except for the tumbling motion of the 11EB1M7 smectogen, in which a sensible jump has been observed.

These results confirm that most of the differences in the dynamics behavior between the SmA and SmC* phases are not in the fast-regime of motion, and they are not due to single-molecule motions. On the contrary, in the slow regime, these two mesophases are expected to be quite different due to collective motions, such as soft or goldstone modes, as it has been detected by other experimental techniques [46].

UNUSUAL PROPERTIES IN BANANA-SHAPED LIQUID CRYSTALS

BLCs have been studied by ^{2}H NMR spectroscopy only in recent years. However, the few papers already published confirmed the power of this technique to point out the peculiar properties of these new molecular systems.

For instance, the biaxiality of the nematic phase formed by a BLC has been demonstrated by simulating ^{2}H NMR spectra acquired under specific experimental conditions [20]. This important result has been confirmed by other experimental techniques, such as X-ray diffraction [62], and it represents the first evidence of the existence of the biaxial nematic phase in thermotropic single compounds.

Another example concerns the conformational properties, which are connected with the molecular chirality: the classical method based on the analysis of ^{2}H NMR spectra of molecular probes diluted in liquid-crystalline solvents has been applied to BLC systems [63,64]. These studies performed on both BLC subunits [63,64] and BLCs themselves [65] diluted in common calamitic nematics show that the behavior of bent molecules is completely different if they are in the bulk [13] or if they are used as probes in a calamitic environment [63–65]. In this last case, the average conformation of the BLC molecules is not chiral, due to the very fast reorientation of the two lateral wings around the ester linkages. This finding is in agreement with theoretical calculations [18,66] performed on single molecules, showing that the potential energy surface is characterized by a very flat minimum corresponding to several conformations.

On the contrary, the behavior of bent molecules in the bulk is much more complicated, mainly due to molecular packing. Several studies [17–19,21] confirmed that when bent molecules are packed together as in the B_2 phase, a twisted (chiral) conformation may be assumed by these molecules (see Fig. 4).

Concerning the molecular and geometrical properties of BLCs, the studies performed on two selectively labeled mesogens, the 1,3-phenylene bis{4-4'-(11-undecenyloxy)benzoyloxy} benzoate (Pbis11BB) and its 4-chloro homolog (ClPbis11BB) can be taken as representative. The molecular structure of these BLCs is reported in Fig. 4a, where the bending angle is also shown. This molecular feature is very important in determining the mesophase behavior.

In fact, ^{13}C and ^{2}H NMR results [67], as well as theoretical calculations [66], have shown that if the bending angle is larger than a limiting value, approximately 135/140°, depending on the molecular structure, no B_i phases appear, in favor of the nematic or smectic phases.

This behavior has been confirmed by different experimental and theoretical studies, and it is well accepted by chemists working in the field, as reported in the reviews [5,68,69].

However, the bent shape of these molecules is probably responsible for several other unusual properties, as those observed by ^{2}H NMR relaxation measurements concerning the molecular dynamics [21–23].

The mesogens ClPbis11BB [13,14,21–23] and Pbis11BB [13,21,24], deuterium labeled on their central ring, have been investigated by means of ^{2}H NMR.

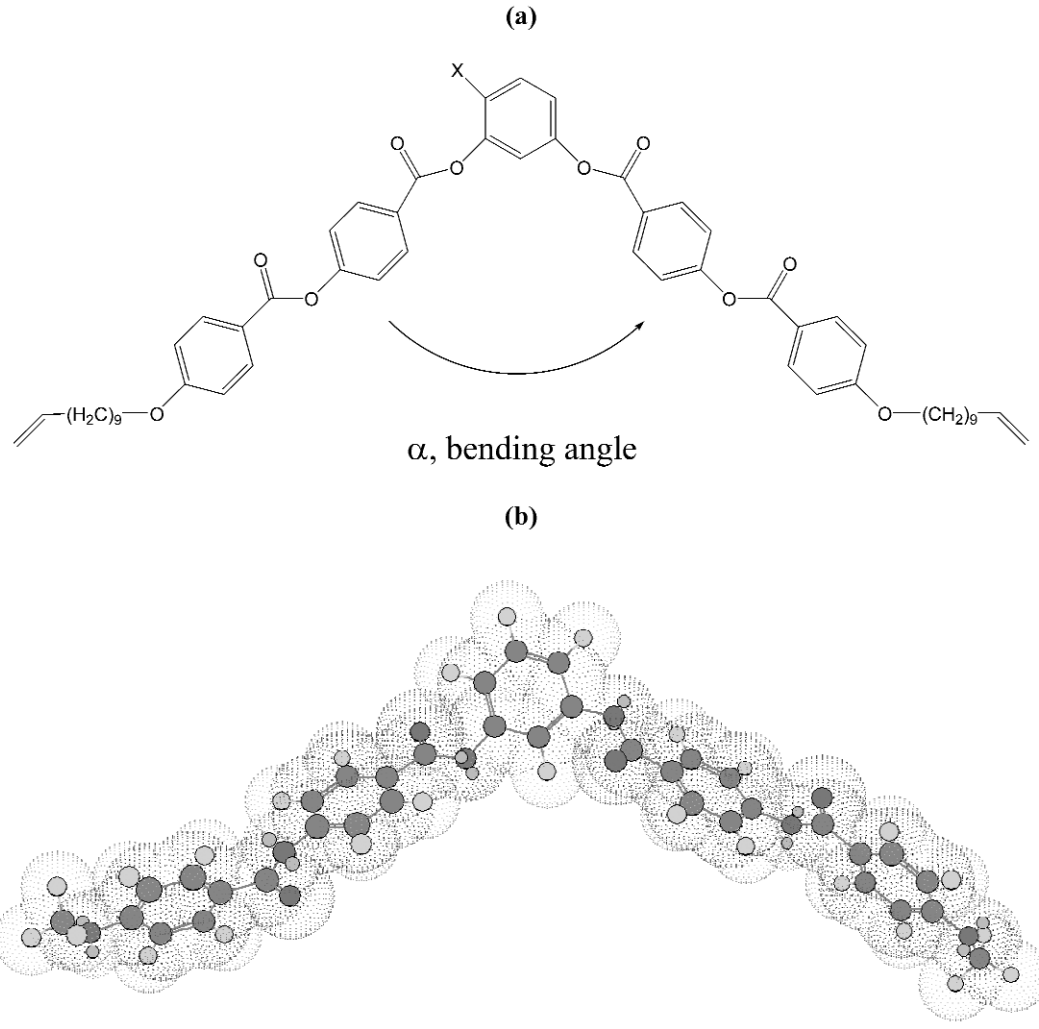

Fig. 4 (a) Molecular structure of the banana-shaped LCs 4-chloro-1,3-phenylene bis{4-4'-(11-undecenyloxy) benzoyloxy} benzoate (ClPbis11BB, X = Cl) and 1,3-phenylene bis{4-4'-(11-undecenyloxy)benzoyloxy} benzoate (Pbis11BB, X = H). (b) Twisted (chiral) conformation of Pbis1BB (five-ring core of the Pbis11BB mesogen) minimized according to ref. [66].

The ^2H line widths and ^2H spin–spin relaxation times T_2 show a trend characterized by the following features, in a wide range of temperatures, from 40° up to the isotropic-mesophase transition temperature to the crystalline phase:

- In the isotropic phase:
  1. The isotropic peak is extremely broad, even at temperatures much higher than the clearing point. This line broadening could not be due to pretransitional effects. Moreover, this anomalous behavior was confirmed by electro-convection [15] and light-scattering measurements [16].
  2. T_2 measurements in the same temperature range reveal that the line broadening is due to dynamics reasons.

3. The analysis of T_2 allows us to estimate the value of the correlation time τ_c ($\approx 10^{-8}$ s) of the motions responsible for this broadening. This correlation time is two orders of magnitude larger than in normal calamitic compounds in their isotropic phase. This means that the motions related to this line broadening are extremely slow respective to conventional isotropic phases [21].

- In the nematic phase:
  1. The observed quadrupolar splitting, $\Delta\nu_q$, is quite large (up to 65 KHz) [13].
  2. The spectral line width is very large (7–8 KHz) [13].
  3. The ^{2}H NMR spectra can be fitted by using simple Lorentzian functions [14], thus demonstrating the dynamic nature of this broadening, which is homogenous. T_2 relaxation time is constant in the nematic range, and its value is about 30 μs (very short respective to common calamitic nematic phases). A qualitative conclusion is that molecules are affected by slow motions in the nematic phase [22].
  4. Quite recently, a molecular model has been developed for identifying the kind of motions responsible for the line broadening. T_2 relaxation times have been analyzed by solving the Louiville stochastic equation [23]. ODFs have been excluded, while the main contribution to the slow dynamics was found to be the overall molecular tumbling motion, with $D_\perp$ smaller than 10^{-6} s. This finding is in agreement with the hypothesis that bent molecules may form local clusters [16] or molecular aggregations [13,14] in the nematic phase.
- In the B_2 phase:
  1. ^{2}H NMR spectra recorded in the B_2 phase of Pbis11BB mesogen, labeled on both central and lateral rings, show that this phase does not align in the magnetic field [24]. The hypothesis is that local smectic domains do form, but in the macroscopic sample, these domains are isotropically distributed, without any preferred orientation.
  2. This behavior is confirmed by ^{13}C NMR too, and it suggests that bent molecules are highly packed in the B_2 phase and that their behavior in the bulk is quite different from that in thin layers, where this phase revealed that it possesses interesting electro-optical properties [68,69].
  3. The fact that bent molecules do not align easily in the magnetic field could be connected with the small value of the magnetic susceptibility anisotropy, as experimental [16] and theoretical studies [13,14] confirm.
  4. Preliminary T_2 relaxation measurements in the B_2 phase confirm that these molecules are affected by slow motions.

CONCLUSION AND FURTHER DEVELOPMENTS

In this paper, some new developments in the field of LCs by means of ^{2}H NMR have been reported. In particular, the dynamics of calamitic LCs in the fast-motion regime has been discussed in detail based on the analysis of a large set of data for several deuterium-labeled smectogens. The values obtained for rotational diffusion coefficients and activation energies for the overall molecular and internal motions reveal that no significant differences exist in the fast-motion regime between the uniaxial SmA and biaxial SmC* phases. However, further developments, including the theoretical treatment of T_2 relaxation times, as well as the comparison with ^{13}C relaxation times and ^{1}H relaxometry, are very promising to get a complete overview of the molecular dynamics of calamitic LCs.

Concerning the new liquid-crystalline phases formed by banana-shaped mesogens, their unique orientational and dynamic properties have been described here, as detected by ^{2}H NMR spectroscopy. Among them, the response of these phases to magnetic fields and the tendency of their constituent molecules to form aggregates and complex supramolecular structures are unexpected and will require further investigations.

In fact, one of the most interesting aspects of these liquid-crystalline systems is the complexity of their mesophase structures and the different ways of packing of the molecules. This last behavior is strongly related to the molecular bent, which is at the basis of the strong molecular interactions, the high dipole moment, and the small magnetic susceptibility anisotropy of these molecules.

On the other hand, ^{2}H NMR studies were the first ones presenting evidence that the very unusual slow dynamics affect not only the typical B phases, but also the nematic and isotropic phases formed by banana-shaped mesogens. Further developments for understanding the origin of the restricted overall molecular motions, found by analyzing T_2 relaxation times, will require the modeling of the local structures formed by these bent molecules in both isotropic and nematic phases. To this aim, the hypothesis of molecular entanglement, as well as molecular clustering, offers an interesting possibility to be further investigated.

ACKNOWLEDGMENTS

I thank IUPAC for the recognition of this research work as well as Prof. Carlo Alberto Veracini for his support and for his constant and stimulant suggestions. I would like to thank Profs. Giancarlo Galli and Edward T. Samulski for their scientific support. Part of this research has been carried out with the funds from MIUR (Italian Ministry of Innovation, University and Research), P.R.I.N. 2003 and P.R.I.N. 2005 projects, and the "Galileo Galilei" Ph.D. School of the University of Pisa.

REFERENCES

1. S. T. Lagerwall. *Ferroelectric and Antiferroelectric Liquid Crystals*, Wiley-VCH, New York (1999).
2. J. W. Goodby, R. Blinc, N. A. Clark, S. T. Lagerwall, M. A. Osipov, S. A. Pikin, T. Sakurai, K. Yoshino, B. Zeks. *Ferroelectric Liquid Crystals, Principle, Properties and Applications*, Gordon and Breach, London (1991).
3. S. Kobayashi. Plenary lecture (PL3) at the 10th Conference on Ferroelectric Liquid Crystals, Stare Jablonki (Poland), 12–17 September 2005.
4. T. Niori, T. Sekine, J. Watanabe, T. Furukawa, H. Takezoe. *J. Mater. Chem.* **6**, 1231 (1996).
5. G. Pelzl, S. Diele, W. Weissflog. *Adv. Mater.* **11**, 707 (1999).
6. R. Y. Dong. *Nuclear Magnetic Resonance of Liquid Crystals*, Springer, New York (1997).
7. R. L. Vold, R. R. Vold. In *The Molecular Dynamics of Liquid Crystals*, Vol. 431, G. R. Luckhurst, C. A. Veracini (Eds.), Chap. 7, NATO ASI Series (1989).
8. V. Domenici, M. Geppi, C. A. Veracini. *Chem. Phys. Lett.* **382**, 518 (2003).
9. V. Domenici, J. Czub, M. Geppi, B. Gestblom, S. Urban, C. A. Veracini. *Liq. Cryst.* **31**, 91 (2004).
10. V. Domenici, M. Geppi, C. A. Veracini, A. V. Zakharov. *J. Phys. Chem. B* **109**, 18369 (2005).
11. W. Zajac, S. Urban, V. Domenici, M. Geppi, C. A. Veracini, M. T. F. Telling, B. J. Gabrys. *Phys. Rev. E* **73**, 051704 (2006).
12. C. A. Veracini. In *Nuclear Magnetic Resonance of Liquid Crystals*, J. W. Emsley (Ed.), Chap. 5, Reidel, Dordrecht (1985).
13. V. Domenici, C. A. Veracini, B. Zalar. *Soft Matter* **1**, 408 (2005).
14. V. Domenici, C. A. Veracini, G. Prampolini, I. Cacelli, A. Lebar, B. Zalar. To be submitted for publication.
15. D. Wiant, J. T. Gleeson, N. Eber, K. Fodor-Csorba, A. Jakli, T. Toth-Katona. *e-Liq. Cryst. Comm., Phys. Rev. E* **72**, 041712 (2005).
16. D. Wiant, S. Stojadinovic, K. Neupane, S. Sharma, K. Fodor-Csorba, A. Jakli, J. T. Gleeson, S. Sprunt. *e-Liq. Cryst. Comm., Phys. Rev. E* **73**, 030703 (2006).
17. H. Kurosu, M. Kawasaki, M. Hirose, M. Yamada, S. Kang, J. Thisayukta, M. Sone, H. Takezoe, J. Watanabe. *J. Phys. Chem. A* **108**, 4674 (2004).

18. T. Imase, S. Kawauchi, J. Watanabe. *J. Mol. Struct.* **560**, 275 (2001).
19. K. Fodor-Csorba, A. Vajda, G. Galli, A. Jakli, D. Demus, S. Holly, E. Gacs-Baitz. *Macromol. Chem. Phys*. **203**, 1556 (2000).
20. L. A. Madsen, D. J. Digemans, M. Nakata, E. T. Samulski. *Phys. Rev. Lett.* **92**, 145505 (2004).
21. V. Domenici, M. Geppi, C. A. Veracini, A. Lebar, B. Zalar, R. Blinc. *J. Phys. Chem. B* **109**, 469 (2005).
22. V. Domenici, K. Fodor-Csorba, D. Frezzato, G. Moro, C. A. Veracini. *Ferroelectrics* **344**, 19 (2006).
23. V. Domenici, D. Frezzato, C. A. Veracini. *J. Phys. Chem. B* In press.
24. J. Xu, R. Y. Dong, V. Domenici, K. Fodor-Csorba, C. A. Veracini. *J. Phys. Chem. B* **110**, 9434 (2006).
25. M. E. Rose. *Elementary Theory of Angular Momentum*, John Wiley, New York (1957).
26. R. Y. Dong. *Nuclear Magnetic Resonance of Liquid Crystals*, Chap. 3, pp. 53–64, Springer, New York (1997).
27. C. Zannoni. In *Nuclear Magnetic Resonance of Liquid Crystals*, Vol. 141, J. W. Emsley (Ed.), Chaps. 1 and 2, NATO ASI Series, Reidel, Dordrecht (1985).
28. A. Saupe. *Z. Naturforsch., A* **19**, 161 (1965).
29. G. Vertogen, W. H. De Jeu. *Thermotropic Liquid Crystals, Fundamentals*, Springer-Verlag, Amsterdam (1987).
30. A. Abragram. *Principles of Nuclear Magnetism*, Oxford University Press, London (1961).
31. J. W. Emsley, J. C. Lindon. *NMR Spectroscopy Using Liquid Crystal Solvent*, Pergamon Press, Oxford (1975).
32. (a) E. T. Samulski. In *NMR of Ordered Liquids*, E. E. Burnell, C. A. de Lange (Eds.), Chap. 13, Kluwer Academic, Dordrecht (2003); (b) D. J. Photinos. In *NMR of Ordered Liquids*, E. E. Burnell, C. A. de Lange (Eds.), Chap. 12, Kluwer Academic, Dordrecht (2003).
33. G. L. Hoatson, Y. K. Levine. In *The Molecular Dynamics of Liquid Crystals*, Vol. 431, G. R. Luckhurst, C. A. Veracini (Eds.), Chap. 1, NATO ASI Series (1989).
34. R. Y. Dong. *Prog. Nucl. Magn. Reson. Spectrosc.* **41**, 115 (2002).
35. J. W. Doane. In *Nuclear Magnetic Resonance in Liquid Crystals*, Vol. 141, J. W. Emsley (Ed.), Chap. 16, NATO ASI Series (1983).
36. G. Kothe, J. Stohrer. In *The Molecular Dynamics of Liquid Crystals*, Vol. 431, G. R. Luckhurst, C. A. Veracini (Eds.), Chap. 8, NATO ASI Series (1989).
37. J. H. Davis, K. R. Jeffrey, M. Bloom, M. I. Valic, T. P. Higgs. *Chem. Phys. Lett.* **42**, 390 (1976).
38. R. Blinc, H. Hogenboom, D. O'Reilly, E. Peterson. *Phys. Rev. Lett*. **23**, 969 (1969).
39. Z. Luz, S. Meiboom. *J. Chem. Phys*. **39**, 366 (1963).
40. D. Catalano, L. Chiezzi, V. Domenici, M. Geppi, C. A. Veracini. *J. Phys. Chem. B* **107**, 10104 (2003).
41. D. Catalano, C. Forte, C. A. Veracini, J. W. Emsley, G. N. Shilstone. *Liq. Cryst.* **2**, 345 (1987).
42. D. Catalano, L. Chiezzi, V. Domenici, R. Y. Dong, K. Fodor-Csorba, M. Geppi, C. A. Veracini. *Macromol. Chem. Phys*. **203**, 1594 (2002).
43. D. Catalano, M. Cifelli, K. Fodor-Csorba, M. Geppi, E. Gaics-Baitz, A. Jakli, C. A. Veracini. *Mol. Cryst. Liq. Cryst.* **351**, 245 (2000).
44. D. Catalano, M. Cavazza, L. Chiezzi, M. Geppi, C. A. Veracini. *Liq. Cryst.* **27**, 621 (2000).
45. D. Catalano, M. Cifelli, V. Domenici, K. Fodor-Csorba, R. Richardson, C. A. Veracini. *Chem. Phys. Lett.* **346**, 259 (2001).
46. I. Musevic, R. Blinc, B. Zeks. *The Physics of Ferroelectric and Antiferroelectric Liquid Crystals*, World Scientific, London (2000).
47. V. Domenici, M. Geppi, C. A. Veracini. *Prog. Nucl. Magn. Reson. Spectrosc.* In press.
48. A. G. Redfield. *Adv. Magn. Reson.* **1**, 1 (1965).
49. P. L. Nordio, P. Busolin. *J. Chem. Phys.* **55**, 5485 (1971).

50. D. E. Woessner. *J. Chem. Phys*. **36**, 1 (1962).
51. R. Y. Dong. *Mol. Cryst. Liq. Cryst*. **141**, 349 (1986).
52. P. A. Beckmann, J. W. Emsley, G. R. Luckurst, D. L. Turner. *Mol. Phys*. **59**, 97 (1986).
53. R. Y. Dong. *Mol. Phys*. **88**, 979 (1996).
54. L. Calucci, M. Geppi. *J. Chem. Inf. Comput. Sci.* **41**, 1006 (2001).
55. D. Catalano, M. Cifelli, M. Geppi, C. A. Veracini. *J. Phys. Chem. A* **105**, 34 (2001).
56. F. Perrin. *J. Phys. Radium* **5**, 497 (1934).
57. M. Cifelli, C. Forte, M. Geppi, C. A. Veracini. *Mol. Cryst. Liq. Cryst.* **372**, 81 (2001).
58. L. Chiezzi, V. Domenici, M. Geppi, C. A. Veracini, R. Y. Dong. *Chem. Phys. Lett*. **358**, 257 (2002).
59. R. Y. Dong, J. Zhang, C. A. Veracini. *Solid State NMR* **28**, 173 (2005).
60. V. Domenici, M. Geppi, C. A. Veracini, R. Blinc, A. Lebar, B. Zalar. *ChemPhysChem* **5**, 559 (2004).
61. V. Domenici, M. Geppi, C. A. Veracini, R. Y. Dong. *Liq. Cryst.* **33**, 479 (2006).
62. B. R. Acharya, A. Primak, S. Kumar. *Phys. Rev. Lett.* **92**, 145506 (2004).
63. V. Domenici, L. A. Madsen, E. J. Choi, E. T. Samulski, C. A. Veracini. *Chem. Phys. Lett.* **402**, 388 (2005).
64. V. Domenici, C. A. Veracini. *Mol. Cryst. Liq. Cryst.* Accepted for publication.
65. G. Cinacchi, V. Domenici. *Phys. Rev. E* **74**, 030701(R) (2006).
66. I. Cacelli, G. Prampolini. *Chem. Phys*. **314**, 283 (2005).
67. R. Y. Dong, K. Fodor-Csorba, V. Domenici, J. Xu, G. Prampolini, C. A. Veracini. *J. Phys. Chem. B* **108**, 7694 (2004).
68. R. A. Reddy, C. Tschierske. *J. Mater. Chem*. **15**, 1 (2005).
69. H. Takezoe, Y. Takanishi. *Jpn. J. Appl. Phys., Part 1* **45**, 597 (2006).